# MICROSTRUCTURE AND THERMAL CHARACTERIZATION OF Mo-DOPED $Li_{6.87}Nb_{2.34}Ti_{5.78}O_{21}$ SOLID-SOLUTION CERAMICS

**Tamara Ivetić**[1], **Jelena Petrović**[2], **Imre Gúth**[1], **Kristina Čajko**[1], **Svetlana Lukić-Petrović**[1]

*[1]University of Novi Sad Faculty of Sciences, Department of Physics, Trg Dositeja Obradovića 4, 21000 Novi Sad, Serbia*
*[2]Institute for Electronic Appliances and Circuits, Faculty Computer Science and Electrical Engineering, University of Rostock, Albert-Einstein 2, 18059, Rostock, Germany*
*e-mail: tamara.ivetic@df.uns.ac.rs*

## Abstract

In this work, the microstructure and thermal properties of lithium-niobium-titanium-oxide (Li-Nb-Ti-O) solid-solution ceramics were investigated using the X-ray diffraction (XRD), Raman spectroscopy, scanning electron microscopy (SEM), and differential scanning calorimetry (DSC) techniques. XRD and SEM analysis confirmed that Li-Nb-Ti-O ceramic sample synthesized by solid-state method reaches the desired composition of so-called M-phase of the $Li_2O$-$Nb_2O_5$-$TiO_2$ ternary system ($Li_{6.87}Nb_{2.34}Ti_{5.78}O_{21}$) that should have excellent microwave dielectric properties. The M-phase was obtained with lower than 1000ºC sintering temperature by doping with $MoO_3$ as flux material, which makes this kind of ceramic material suitable for the low temperature co-fired ceramic (LTCC) technology applications. The heat flow data obtained from DSC measurement were used to calculate the specific heat capacity ($C_p$) of synthesized $Li_{6.87}Nb_{2.34}Ti_{5.78}O_{21}$ solid-solution ceramics, which is the property of a material that tells about its stability and functionality.

## Introduction

The modern wireless communications, such as mobile systems and its technology, is always searching for ways to miniaturize the mobile device's size. The LTCC technology offers the possibility of fabricating the highly integrated substrates and radio-frequency microwave circuits using a special combination of the ceramic materials and multi-layer/firing techniques. Co-fired ceramic devices are made by processing several layers independently which are assembled into a device as a final step. This allows co-firing the highly conductive materials (like silver) with passive ceramic elements (resistors, capacitors, and inductors). Silver is often used as a metallic electrode in such electrical systems because of its high conductivity and low cost. However, as Ag melting point is low (about 961 ºC) the dielectric ceramics used in the co-fired technology with silver has to have besides the required dielectric properties for the desired application also a low sintering temperature [1]. The ternary $Li_2O$-$Nb_2O_5$-$TiO_2$ material system has been an attractive potential candidate for the LTCC applications for many years now. Especially, its so-called M-phase, which is described by the general formula $Li_{1+x-y}Nb_{1-x-3y}Ti_{x+4y}O_3$ ($0.05<x<0.3$, $0<y<0.182$). As M-phase ceramics usually needs higher than 1100 ºC synthesis temperature, the small additions of low-melting-temperature-oxides such as $MoO_3$ (795 °C) are added as a flux material to lower the synthesis temperature by mechanisms of liquid-phase sintering [2]. The M-phase compounds refer to the series of solid-solutions in the middle of the $Li_2O$-$Nb_2O_5$-$TiO_2$ ternary phase diagram. The M-phase grows into the large oriented anisotropic plate-like particles. Some describe the M-phase structure as the homologous series of solid-solutions phases (in trigonal crystal symmetry) with commensurate intergrowth $LiNbO_3$ layers separated by a single $[Ti_2O_3]^{2+}$ corundum-type layer. Such M-phase type Li-Nb-Ti-O materials are featured with excellent and tuneable microwave dielectric properties (permittivity from 20 to 80) depending on the applied synthesis method, and the type and concentration of the functional additives used [3].

Various dielectric permittivity values of the dielectric ceramics used in LTCC are equally desirable. For example, the low permittivity dielectric ceramics with the fast signal transmission are used as microwave packaging substrates, while the medium dielectric permittivity (20-50) ceramics are used in the dielectric resonators/filters. Besides, studying the thermal properties of this kind of materials is of great interest as well, because the electronic systems, where these materials find applications, are often exposed to different and frequently extreme environmental conditions. The specific heat capacity and enthalpy change during the melting process were calculated using the obtained heat flow curve from DSC recordings [4].

## Experimental

The Li-Nb-Ti-O ceramic sample was synthesized using a solid-state method. Starting precursors, the commercial powders of anatase $TiO_2$, $Nb_2O_5$, and $LiCO_3$ (all purchased from Sigma-Aldrich), were mixed in a molar ratio to reach the desired composition with the addition of not more than 0.5 wt. % of $MoO_3$ (sample is further marked in the text as Li-Nb-Ti-O-Mo). The mixed powders were milled in the planetary ball mill (Retsch GmbH PM100) in zirconia vial and by zirconia balls of 5 mm diameter. The ball milling was performed in ethanol for 4 h with the use of standard balls to powder mass ratio of 10:1 and 100 rpm speed rate. The obtained powder mixture was dried on air for 24 h and calcinated at 650 °C for 4h. The mechanically activated powder mixture was pressed by 10 mm diameter mold to form stable pellet that was finally sintered at 900 °C for 4h. XRD analysis was used for structural characterization and was performed on a MiniFlex600 (Rigaku, Japan) X-ray diffractometer with Cu-$K_\alpha$ radiation ($\lambda = 1.5406$ Å) at a tube voltage of 40 kV and a tube current of 15 mA, with steps of 0.02° and a counting time of 1°/min, in the $2\theta$ angular range from 10° to 80°. With scanning electron microscope (JEOL JSM-6460LV), the morphology of the sample was investigated. The Raman spectrum was measured using the Centice MMS Raman spectrometer equipped with a CCD detector and a diode laser, operating at 785 nm (1.58 eV) with the power of 70 mW, as the excitation source. Non-isothermal differential scanning calorimetry (DSC) measurements were performed using NETZSCH STA 449 F3 Jupiter, equipped with DSC sample holders and using $Al_2O_3$ crucibles and samples in a powder form with a mass around 20 mg in an inert atmosphere of $N_2$ with a control flow rate of 20 ml/min. Temperature and heat flow calibration was performed for all the heating/cooling rates used in this research. Specific heat capacity measurements procedure used a sapphire crystal as reference material. The heating started at room temperature up to 40 ºC with a hold for 30 min, then the heating continued up to 1200 ºC with a heating rate of 10 K/min and hold for 30 min before the final cooling to room temperature.

## Results and discussion

The obtained Li-Nb-Ti-O-Mo sample microstructure (Fig. 1) is characterized by the plate-like particles that strongly resemble the microstructure already described for the M-phase materials [1]. The obtained XRD result (Fig. 2) supports results from SEM findings (Fig. 1) that M-phase of $LiO_2$-$Nb_2O_3$-$TiO_2$ system was formed. Majority of XRD peaks were indexed according to COD reference card no. 1533457 that describes $Li_{6.87}Nb_{2.34}Ti_{5.78}O_{21}$ solid-solution crystal system with $P\bar{3}c1$ (no. 158) space group symmetry. Few impurity related diffraction peaks belong to $LiNbO_3$ and $TiO_2$ anatase (marked in Fig. 1) and no XRD peaks were found to relate to added $MoO_3$ compound.

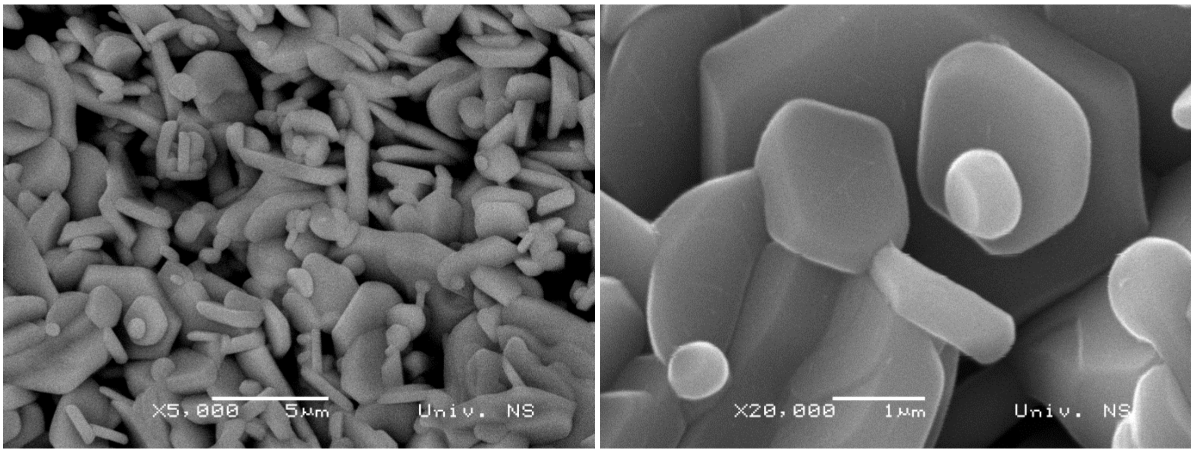

**Figure 1.** SEM images of synthesized Li-Nb-Ti-O-Mo ceramic sample

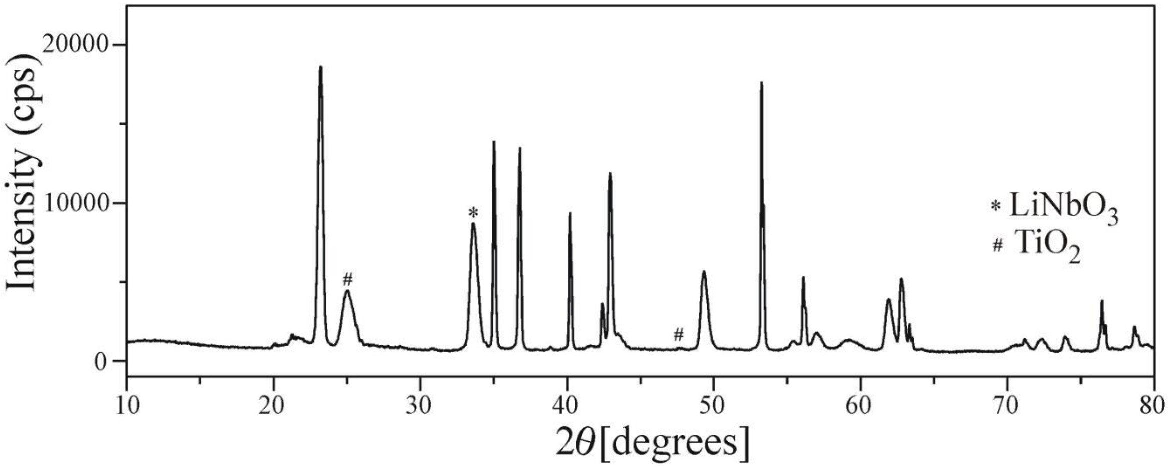

**Figure 2.** XRD pattern of synthesized Li-Nb-Ti-O-Mo ceramic sample

The Raman spectrum obtained by 785 nm excitation wavelength is shown in Fig. 3. The exact Raman peak positions (shift in cm$^{-1}$), intensity (counts) and full width at half maximum (FWHM) were determined by the amplitude version of Gaussian line-shape multi-peak fitting procedure (inset in Fig. 3). There are no past reports, as far as we know, on Raman spectrum for $Li_{6.87}Nb_{2.34}Ti_{5.78}O_{21}$ M-phase in the $P\bar{3}c1$ space group symmetry obtained by 785 nm excitation wavelength.

The DSC curve recorded for Li-Nb-Ti-O-Mo sample is shown in Fig. 4. The DSC spectrum features the endothermic peak at 1177 ºC that characterizes the melting of $Li_{6.87}Nb_{2.34}Ti_{5.78}O_{21}$ compound. There was no change in mass. The DSC recording was used to calculate the specific heat capacity ($C_p$) of $Li_{6.87}Nb_{2.34}Ti_{5.78}O_{21}$. The melting enthalpy ($\Delta H_m$) is calculated as the area below the heat capacity vs. temperature curve in the area where the change of this parameter is significant (the shaded area in the inset in Fig. 4) as $\Delta H_m = \int_{T_1}^{T_2} C_p(T)dt$.

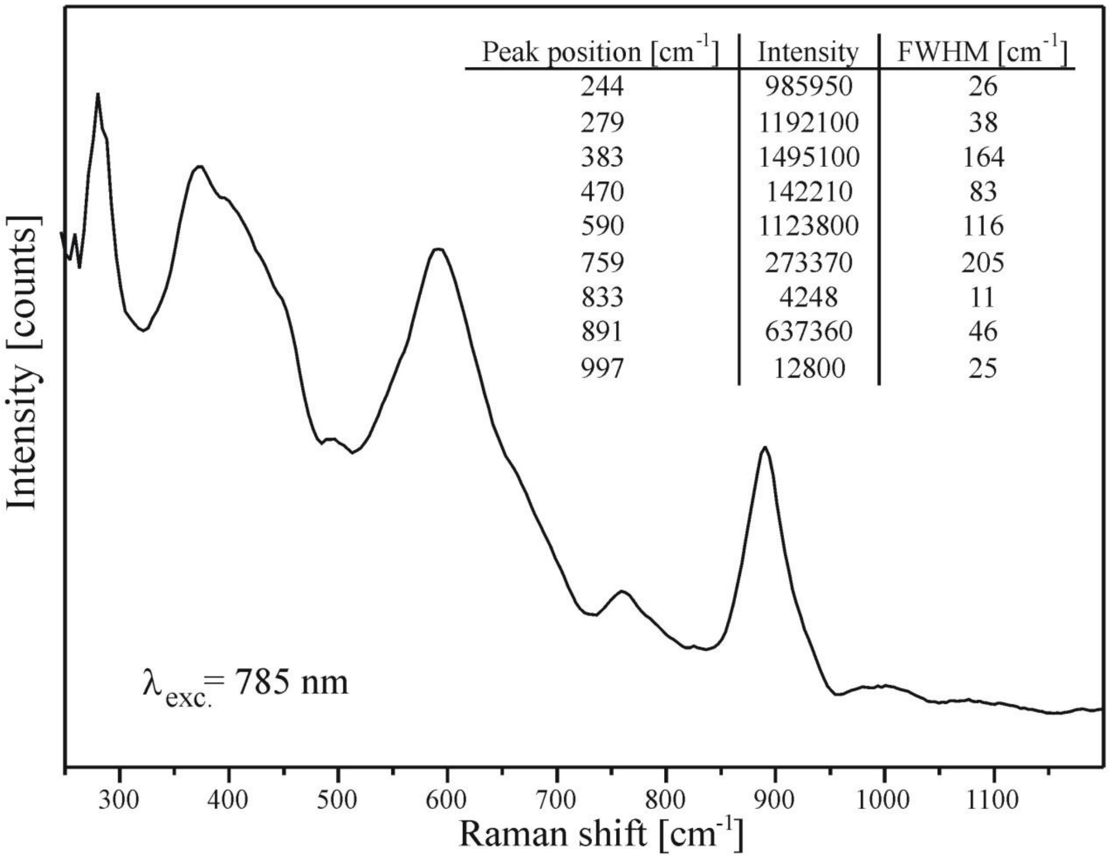

| Peak position [cm$^{-1}$] | Intensity | FWHM [cm$^{-1}$] |
|---|---|---|
| 244 | 985950 | 26 |
| 279 | 1192100 | 38 |
| 383 | 1495100 | 164 |
| 470 | 142210 | 83 |
| 590 | 1123800 | 116 |
| 759 | 273370 | 205 |
| 833 | 4248 | 11 |
| 891 | 637360 | 46 |
| 997 | 12800 | 25 |

**Figure 3.** Raman spectrum of synthesized Li-Nb-Ti-O-Mo ceramic sample at room temperature obtained by 785 nm excitation wavelength

In the case of DSC measurement, the specific heat capacity of the sample at a given temperature and constant pressure, $C_p$, was calculated by a simple comparison of the heat flow rates into the sample and reference material (etalon-sapphire) [5] $C_p = \frac{\Phi_s - \Phi_0}{\Phi_{ref} - \Phi_0} \cdot \frac{m_{ref}}{m_s} C_p^{ref}$, where $\Phi_s$, $\Phi_{ref}$ and $\Phi_0$ represent heat flow rates through crucible loaded with sample material, crucible loaded with reference material and empty crucible, respectively. $m_s$ and $m_{ref}$ represent the mass of the sample and reference material respectively, while $C_p^{ref}$ is the specific heat capacity of the reference material. Values for the heat capacity of sapphire between 200 °C to 2200 °C, required for specific heat calculation, are available in the NETZSCH Proteus software suite. The variation of the heat capacity with the temperature in $Li_{6.87}Nb_{2.34}Ti_{5.78}O_{21}$ crystalline solid is characterized by the melting temperature of 1177 ºC and its belonging heat capacity maximum of $C_p$ = 18.7 J/gK (shown as an inset in Fig. 4). By integrating the $C_p$ melting peak area, the enthalpy change per unit weight of approximately $\Delta H_m$ = 364.7 J/g was calculated for this thermal event (inset in Fig. 4).

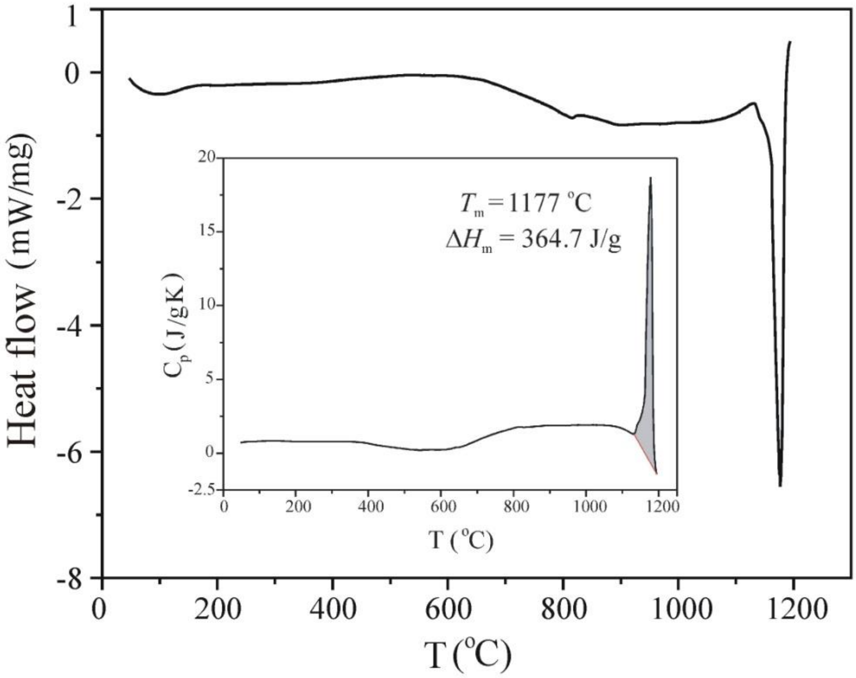

**Figure 4.** DSC curve of $Li_{6.87}Nb_{2.34}Ti_{5.78}O_{21}$ ceramic sample (inset shows the calculated variation of the specific heat capacity ($C_p$) with the temperature)

## Conclusion

In this work, the Li-Nb-Ti-O ceramic was synthesized by the solid-state method and its microstructure and thermal properties were investigated. Synthesized Li-Nb-Ti-O is specially featured by 900 ºC synthesis temperature (achieved by adding $MoO_3$ as flux material) and M-phase like superstructure, which makes it applicable for the LTCC technology. The microstructure analysis confirmed the formation of a member of the M-phase wherein the general formula $Li_{1+x-y}Nb_{1-x-3y}Ti_{x+4y}O_3$, the $x = 0.12$ and $y = 0.18$ give the final composition of ~$LiNb_{0.34}Ti_{0.84}O_3$ which is equal to $Li_{6.84}Nb_{2.34}Ti_{5.78}O_{21}$ found by XRD. The results presented here give a good starting insight into the possible use of this kind of material. Exploring the obtained Li-Nb-Ti-O ceramics needs further electrical characterization, which will give a complete picture of the applicability of this material in the modern electrical devices.

## Acknowledgments

This work was financially supported by the APV Provincial Secretariat for Higher Education and Scientific Research (project name: “Properties and electrical characteristics of doped amorphous chalcogenide materials and nanostructured ceramics”, project number: 142-451-2080/2019-04), and the Ministry of Education, Science and Technological Development of the Republic of Serbia (project number ON 171022).

## References

[1] Z. Liu, Y. Wang, W. Wu, Y. Li, J. Asian Ceram. Soc. 1 (2013) 2.
[2] D. Zhou, C.A. Randall, H. Wang, L-X. Pang, X. Yao, J. Am. Ceram. Soc. 93 (2010) 1096.
[3] H-F. Zhou, H. Wang, D. Zhou, L-X. Pang, X. Yao, Mater. Chem. Phys. 109 (2008) 510.
[4] E. Morîntale, A. Harabor, C. Constantinescu, P. Rotaru, Physics AUC 23 (2013) 89.
[5] G.W.H. Höhne, W. Hemminger, H.-J. Flammersheim, Differential Scanning Calorimetry: An Introduction for Practitioners, Springer, Berlin, 1996.